Eidgenössische Technische Hochschule Zürich
Swiss Federal Institute of Technology Zurich

PAUL SCHERRER INSTITUT

Crystalline Ion Beams
A Group Theoretical Approach

Semester Project

in Accelerator Physics

Department of Physics

ETH Zurich

written by

Vitus Ilmo Getzinger

supervised by

Dr. A. Adelmann (ETH)

September 19, 2024

Eidgenössische Technische Hochschule Zürich
Swiss Federal Institute of Technology Zurich

Eigenständigkeitserklärung

Die unterzeichnete Eigenständigkeitserklärung ist Bestandteil jeder während des Studiums verfassten schriftlichen Arbeit. Eine der folgenden drei Optionen ist in Absprache mit der verantwortlichen Betreuungsperson verbindlich auszuwählen:

☒ Ich bestätige, die vorliegende Arbeit selbständig und in eigenen Worten verfasst zu haben, namentlich, dass mir niemand beim Verfassen der Arbeit geholfen hat. Davon ausgenommen sind sprachliche und inhaltliche Korrekturvorschläge durch die Betreuungsperson. Es wurden keine Technologien der generativen künstlichen Intelligenz[1] verwendet.

☐ Ich bestätige, die vorliegende Arbeit selbständig und in eigenen Worten verfasst zu haben, namentlich, dass mir niemand beim Verfassen der Arbeit geholfen hat. Davon ausgenommen sind sprachliche und inhaltliche Korrekturvorschläge durch die Betreuungsperson. Als Hilfsmittel wurden Technologien der generativen künstlichen Intelligenz[2] verwendet und gekennzeichnet.

☐ Ich bestätige, die vorliegende Arbeit selbständig und in eigenen Worten verfasst zu haben, namentlich, dass mir niemand beim Verfassen der Arbeit geholfen hat. Davon ausgenommen sind sprachliche und inhaltliche Korrekturvorschläge durch die Betreuungsperson. Als Hilfsmittel wurden Technologien der generativen künstlichen Intelligenz[3] verwendet. Der Einsatz wurde, in Absprache mit der Betreuungsperson, nicht gekennzeichnet.

Titel der Arbeit:

Crystalline Ion Beams – A Group Theoretical Approach

Verfasst von:
Bei Gruppenarbeiten sind die Namen aller Verfasserinnen und Verfasser erforderlich.

Name(n):	**Vorname(n):**
Getzinger	Vitus Ilmo

Ich bestätige mit meiner Unterschrift:
- Ich habe mich an die Regeln des «Zitierleitfadens» gehalten.
- Ich habe alle Methoden, Daten und Arbeitsabläufe wahrheitsgetreu und vollständig dokumentiert.
- Ich habe alle Personen erwähnt, welche die Arbeit wesentlich unterstützt haben.

Ich nehme zur Kenntnis, dass die Arbeit mit elektronischen Hilfsmitteln auf Eigenständigkeit überprüft werden kann.

Ort, Datum	**Unterschrift(en)**
Zürich, 06.07.2024	

Bei Gruppenarbeiten sind die Namen aller Verfasserinnen und Verfasser erforderlich. Durch die Unterschriften bürgen sie grundsätzlich gemeinsam für den gesamten Inhalt dieser schriftlichen Arbeit.

[1] z. B. ChatGPT, DALL E 2, Google Bard
[2] z. B. ChatGPT, DALL E 2, Google Bard
[3] z. B. ChatGPT, DALL E 2, Google Bard

Acknowledgment

I would like to express my deep gratitude to Dr. Andreas Adelmann for his patience and most valuable feedback. Furthermore, I am grateful to Laura Schüpke, Alexia Getzinger and Günter Getzinger. Thank you for motivating and supporting me during the past months.

Nomenclature

$\|G\|$	Order of group G
α	Breaking constant of cooling force
$\chi_j(g)$	Trace of representation j under group element g
ΔT	Difference between temperature and critical temperature
η	Order parameter
Γ	Natural with of state
γ	Relativistic factor
λ	Dimensionless density of crystalline beams
$\|\cdot\|$	Euclidean norm in cartesian coordinates
$\|\cdot\|_a$	Euclidean norm in accelerator coordinates
Φ	Thermodynamic potential
σ_h	Reflection about xy-plane
σ_v	Reflection about a vertical plane
σ_{xy}	Reflection about xy-plane
$\vec{x}_n$	Position vector of the n-th particle
a	Separation between two consecutive particles
c	Speed of light
$C_n(x)$	n-fold rotation about x-axis
E	Identity operation
I	Inversion
k	Number of strings of a helix sharing the same z-positions
k'	Spring constant of confining force
m	Particle mass
N	Total number of particles
n	Number of strings of a helix
P_α	Projector onto the α-th irreducible representation
$p_{n,i}$	Momentum of the n-th particle (i coordinate)
Q	Electric charge of particle
R	Radius of the toroidal confinement
S_n	n-fold rotoreflection
x_n	x position of the n-th particle

Abstract

We attempt to describe crystalline beams from a group theoretical perspective. To achieve this, we first take a closer look on the formation process of crystalline beams for which we propose an approximation for the electric field of helical crystals - of the form $E_{helix} \approx CE_{zylinder}$ - and investigate the stability of different helices. Following this, a group theoretical approach will be taken in order to determine the point groups of different crystalline phases. By giving a short introduction to Landau's theory of phase transitions, we will propose a method to explain why phase transitions show up at specific densities. Finally, some of our results will be tested using numeric methods.

1 Introduction

1.1 What are crystalline beams?

Crystalline beams are a cold structure consisting of charged particles, for example ions or molecules, which remain in their crystal state, while moving at constant velocity. The crystals ordered state arises from an external focusing force, which needs to balance the overall coulomb repulsion of the ensemble. While undergoing the phase transition between their liquid and crystalline state, particles arrange themselves energetically optimal, which results in periodic patterns. Furthermore, when being created, ion beams are exposed to both longitudinal and transversal cooling forces in order to reach temperatures low enough to undergo the phase transition into their crystalline state. Usually, a combination of electron and Doppler cooling is used to achieve this. Depending on the specific parameters of the system, particles arrange themselves into different patterns: a string with equidistant spacing, a Zigzag pattern or a helical formation [Rug00].

1.2 Where do we stand now?

Crystalline ion beams were extensively studied in the years following the early 1980s. The first breakthrough marked the NAP-M storage ring in Novosibirsk where the longitudinal velocity spread of electron cooled protons displayed a sudden narrow peak after dropping beneath a critical temperature. It was suggested that the particles entered an ordered state, which was then examined by various groups using numeric methods. Following this, an uprise in the development of high energy storage rings and new cooling mechanisms started. Although the creation of stationary crystals did not prove to be an issue - they can be created in radio-frequency quadrupole ion traps -, crystalline beams offered a different challenge. Despite all efforts, storage ring specific heating mechanisms prevented crystallisation in heavy ion storage rings [SH04]. These studies came to an end in 2002, when U. Schramm, T. Schätz and D. Habs demonstrated the crystallisation of laser cooled, singly positively charged, magnesium ions (Mg^+) in the table-top circular radio frequency storage ring PALLAS in Munich. The resulting beam traveled at a velocity of 2800 $\mathrm{m\,s^{-1}}$ with an astonishing stability, resulting in a total of 3000 revolutions while maintaining the crystalline state [SSH01].

With the recent development of quantum computers, ion traps, as a possibility for qubits to be stored and processed, became more and more of interest. The most advanced systems at the moment, however, allow only for the storage of several dozen ions to be used as qubits [Bru+19] [Ren15]. This limiting factor shone a new light on crystalline beams. Their exceptional stability, regularity and scalability provided a promising alternative to stationary ion traps [SSH01]. For this reason we attempt to summarize some of the main results discovered in the quest for crystalline beams, dive deeper into the topic of crystallography and phase transitions and present our results using numeric methods.

2 Hamiltonians and Equations of motion

In the following two sections, two cases of crystalline ion beams will be discussed: beams in a zylindric and a toroidal confinement. Both cases will be treated from a laboratory reference frame.

For the linear crystal in the cylindric confinement, we will consider infinitely many point charges in cartesian coordinates. The circular crystal in the toroidal confinement, on the other hand, consists of N particles in an accelerator reference frame; $x, y, z \rightsquigarrow x, y, s$. Both crystals will be exposed to two forces,

$$\vec{F}_{break}(\vec{v}) = -\alpha \begin{pmatrix} v_x \\ v_y \\ 0 \end{pmatrix} \text{ and } \vec{F}_{spring}(\vec{x}) = -k' \begin{pmatrix} x \\ y \\ 0 \end{pmatrix},$$

where the last component of both vectors is in the z-direction for the linear crystal and the s-direction for the circular crystal respectively. The first of these insures the transversal cooling of the beam, the second is a focusing force toward the center of the beam. Non relativistic considerations, neglecting the curvature of the torus and assuming the beam to be in equilibrium results in the following Hamiltonians:

$$H = \sum_{n=1}^{\infty} \frac{1}{2m}(p_{n,x}^2 + p_{n,y}^2 + p_{n,z}^2) - \frac{k'}{2}(x_n^2 + y_n^2) + \frac{1}{4\pi\varepsilon_0} \sum_{j>n} \frac{Q^2}{\|\vec{x}_n - \vec{x}_j\|}, \tag{1}$$

$$H = \sum_{n=1}^{\infty} \frac{1}{2m}(p_{n,x}^2 + p_{n,y}^2 + p_{n,s}^2) - \frac{k'}{2}(x_n^2 + y_n^2) + \frac{1}{4\pi\varepsilon_0} \sum_{j>n} \frac{Q^2}{\|\vec{x}_n - \vec{x}_j\|_a}. \tag{2}$$

For the linear crystal we will also provide the relativistic Hamiltonian, by assuming that all particles travel along the z-direction with the same velocity:

$$H = \sum_{n=1}^{\infty} c\sqrt{m^2c^2 + p_{n,x}^2 + p_{n,y}^2 + p_{n,z}^2} - \frac{k'}{2}(x_n^2 + y_n^2) + \frac{1}{4\pi\varepsilon_0} \sum_{j>n} \frac{Q^2\gamma}{\sqrt{(x_n - x_j)^2 + (y_n - y_j)^2 + \gamma^2(z_n - z_j)^2}}.$$

Since all further calculations were done in the non-relativistic regime, we will restrict ourselves to the first two Hamiltonians. Also, for simplification, we used $\varepsilon_0 = 1$ for all further calculations. The resulting equations of motions are as follows:

$$m\ddot{\vec{x}}_n = -k'(x_n\hat{e}_x + y_n\hat{e}_y) + \frac{1}{4\pi} \sum_{j\neq n} \frac{Q^2(\vec{x}_n - \vec{x}_j)}{\|\vec{x}_n - \vec{x}_j\|^3}, \tag{3}$$

$$m\ddot{\vec{x}}_n = -k'(x_n\hat{e}_x + y_n\hat{e}_y) + \frac{1}{4\pi} \sum_{j\neq n} \frac{Q^2(\vec{x}_n - \vec{x}_j)}{\|\vec{x}_n - \vec{x}_j\|_a^3}. \tag{4}$$

2.1 Stability analysis

If the focusing constant k' is high enough, the particles will remain in a 1-dimensional string with equal spacing a, with N the number of particles. If, however, particles are perturbed from their 1-dimensional equilibrium positions and the focusing force is decreased, a 2-dimensional "Zigzag" pattern emerges. Half of the particles - belonging to one string - will shift to a position x, while the remaining particles of the second string will end up at $-x$. For each of the strings, the particles will be separated by a. Also, one of the strings may be shifted along the z-axis by a distance a. In equilibrium, the equation of motion for the particle located at $z = 0$, the above equation of motion is:

$$m\ddot{x} + k'x - 2\frac{Q^2}{4\pi} \sum_{j=1,odd}^{\infty} \frac{2x}{\sqrt{4x^2 + j^2a^2}^3} = 0.$$

For small x and by substituting the Riemann-Zeta function $\zeta(n)$, one finds the expression:

$$m\ddot{x} + x\left[k' - \frac{7Q^2}{8\pi a^3}\zeta(3)\right] = 0.$$

This gives the following stability region for the 1-dimensional crystal [Cha02]:

$$k' > \frac{7Q^2}{8\pi a^3}\zeta(3).$$

Using the same procedure, the following generalised formula for the equation of motion of the 0th particle - located at $\vec{x} = (x, 0, 0)$ - in a helix, consisting of $n \geq 2$ strings arranged in the shape of a regular polygon with equidistant spacing $\Delta z = a$ between two consecutive particles, can be found:

$$m\ddot{x} + k'x - 2\frac{Q^2}{4\pi} \sum_{\substack{j=1 \\ j \bmod n = i \\ i\neq 0}}^{\infty} \frac{x(1 - cos(i\frac{2\pi}{n}))}{\sqrt{d_i^2(x) + j^2a^2}^3} = 0,$$

$$\text{with } d_i(x) = 2x \cdot sin(\frac{i\pi}{n}).$$

For small x, the stability condition becomes:

$$k' > 2\frac{Q^2}{4\pi} \sum_{i=1}^{n-1} \frac{1 - cos(i\frac{2\pi}{n})}{a^3} \sum_{j=1}^{\infty} \frac{1}{((j-1)n + i)^3}.$$

Following this pattern, a more general result for a helix with n strings, of which the ions of every k strings share the same z-positions, can be derived:

$$m\ddot{x} + k'x - \frac{Q^2}{4\pi} \sum_{j=-\infty}^{\infty} \sum_{i=1}^{k} \sum_{l=0}^{\frac{n}{k}-1} \frac{x(1 - cos(2\pi(\frac{i}{k} + \frac{l}{n})))}{\sqrt{d^2_{i\frac{n}{k}+l}(x) + ((j\frac{n}{k} + l)a)^2}^3} = 0. \tag{5}$$

Here the sums do not go over $l = 0$, $i = k$ and $d_i(x)$ is the same as before.

We will now test how well the electric field of a helix of point charges can be approximated by an infinitely extended and infinitesimal thin cylinder along the z-axis with the same area charge density σ and radius R as the radius of the helix. As a first step, the electric field of an infinite chain of charged particles with spacing a will be approximated by the electric field of an infinitely extended, uniformly charged rod located along the z-axis.

First, we demand the two electric fields to be proportional with proportionality constant C_1 and $\lambda = Q/a$:

$$\frac{Q}{4\pi} \sum_{i=-\infty}^{\infty} \frac{1}{r^2 + i^2 a^2} \stackrel{!}{=} C_1 \frac{\lambda}{2\pi r}.$$

Assuming $r \approx a$ and using the solution of the sum $\sum_i \frac{1}{1+i^2} = \pi coth(\pi)$ gives the result:

$$C_1 = \frac{\pi coth(\pi)}{2}. \tag{6}$$

Moving on, we will consider a helix to consist of n charged rods and compare the electric field to that of an uniformly charged, infinitesimal thin cylinder with equivalent area charge density $\sigma = nQ/2\pi Ra$:

$$\frac{Q}{2\pi a} \sum_{i=1}^{n} \frac{1}{r_i} \stackrel{!}{=} C_2 \frac{\sigma R}{r}.$$

Simplifying and setting $r = qR$ leads to the formula:

$$C_2 = \frac{q}{n} \sum_{i=1}^{n} \frac{1}{\sqrt{1 + q^2 - 2qcos(i\frac{2\pi}{n})}}, \tag{7}$$

where a numeric treatment of the sum gives

$$\sum_{i=1}^{n} \frac{1}{\sqrt{1 + q^2 - 2qcos(i\frac{2\pi}{n})}} \approx \frac{n}{q} + \frac{1.6}{q2^q},$$

which provides us with the final result:

$$C_2 \approx 1 + \frac{1.6}{n2^q}. \tag{8}$$

Using the calculations above, we find that the electric field of a helix with average spacing a can be approximated by:

$$\left\| \vec{E}_{q,n}(r) \right\| \approx \frac{\pi coth(\pi)}{2} (1 + \frac{1.6}{n2^q}) \frac{\sigma R}{r}. \tag{9}$$

Clearly, we have $\lim_{n\to\infty} C_2 = 1$ and $\lim_{q\to\infty} C_2 = 1$. We now present plots to give an intuition about the validity of our approximations:

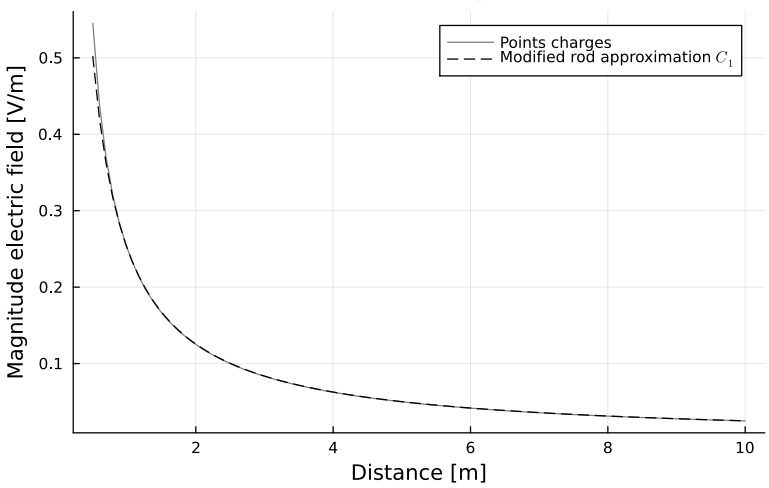

Figure 1: The electric field of an infinitely extended string of charged particles with $Q = 1.0$ C and spacing $a = 1$ m being approximated by a charged rod with equivalent charge density $\lambda = Q/a$ and prefactor C_1 (eq. 6).

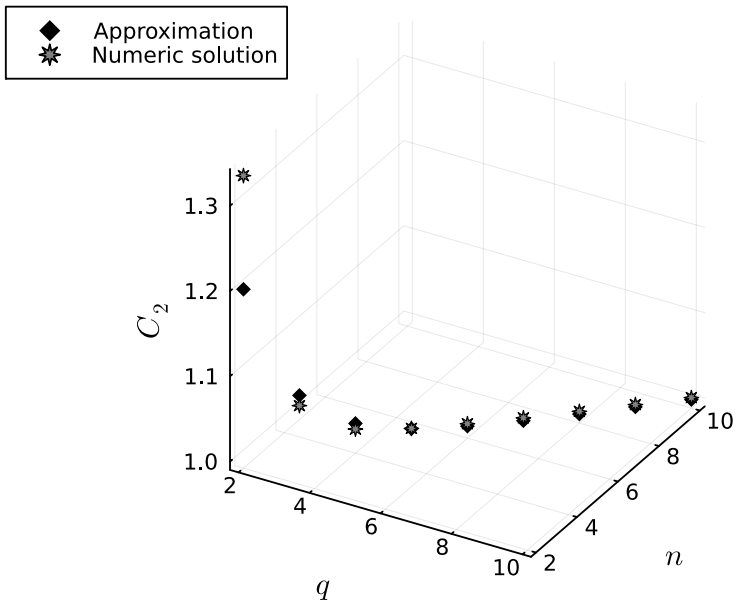

Figure 2: A comparison between the numeric solution of eq. 7 and its approximation (eq. 8) for different n and q.

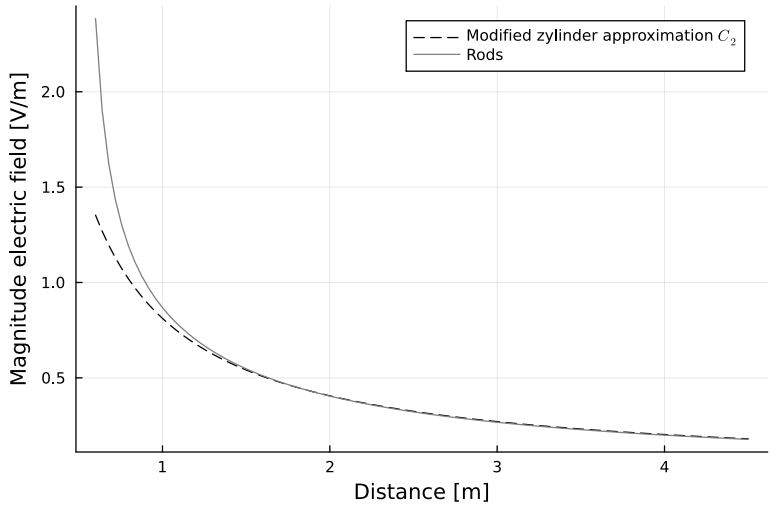

Figure 3: The electric field of $n = 5$ infinitely extended charged rods with $\lambda = 1.0\ \mathrm{C\,m^{-1}}$ each compared to that of an infinitely thin cylinder with equivalent charge density and prefactor C_2.

2.2 Equilibrium analysis

For the single layered helical phase of crystalline beams, we will conduct an investigation on the characteristic lengths of each crystal, in particular their dependence on ion charge Q and focusing constant k'. The characteristic lengths will be the average particle spacing a and average radius r. Afterwards, in figure 6, we present an overview of crystalline structures in dependence of their dimensionless density $\lambda = \frac{1}{a}(3Q^2/2k')^{1/3}$, to display the validity of our simulations. We will not conduct an intensive analysis of the density λ, but want to give an intuitive idea about the shapes of linear crystal beams. To be consistent with prior research, we neglect the factor $1/4\pi$ of eq. 3.

The applied procedure was to vary one of the two parameters at a time and average the desired lengths over all particles:

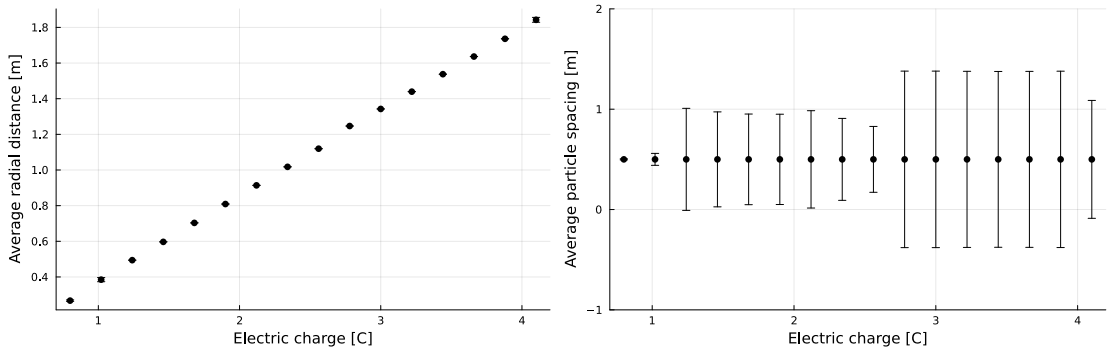

Figure 4: The dependence of a and r on the ions charge Q. A total of $N = 20$ was used, focusing constant was held at $k' = 0.6\ \mathrm{N\,m^{-1}}$. The sudden increase of the error bars in the right plot indicate two phase transitions.

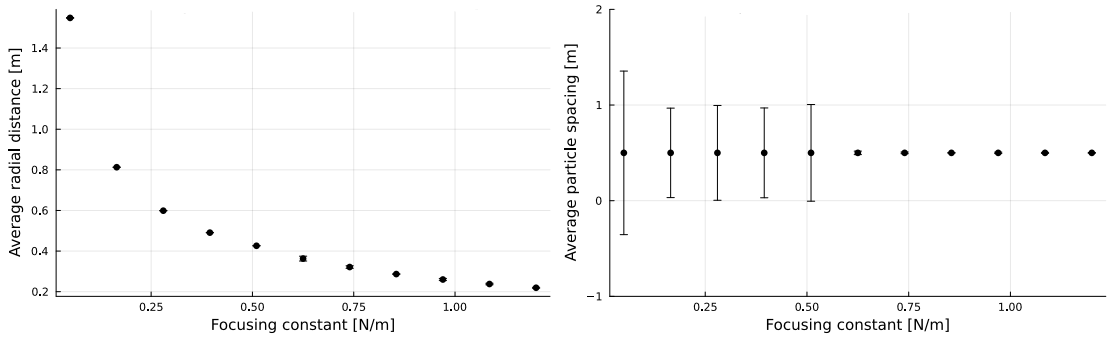

Figure 5: The dependence of a and r on the focusing constant k. A total of $N = 20$ was used, ion charge was held at $Q = 1.0$ C. In the right plot, the sudden decrease of the error bars indicated two phase transitions.

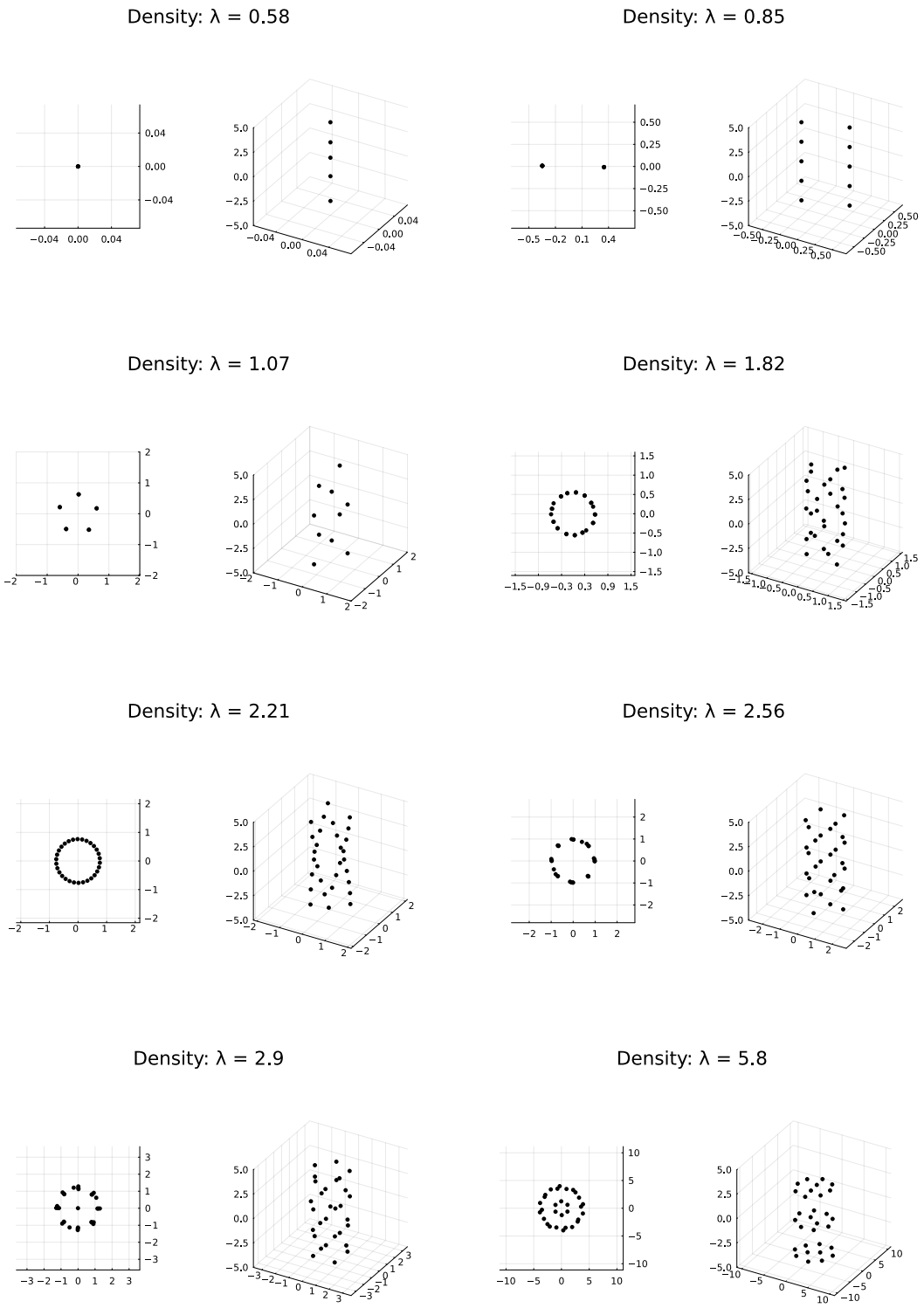

Figure 6: Examples of crystalline beams with dimensionless density $\lambda = \frac{1}{a}(3Q^2/2k')^{1/3}$ with vertical spacing between two consecutive particles a. To avoid overcrowding the plots, the axes (x, y, and z) are not labeled but are in units of meters.

3 Symmetry of crystalline beams

We will discuss the symmetries of three different kinds of crystalline beams - the string, the Zigzag and the helix - by determining the elements contained in the corresponding point groups for each phase. For the following discussion, we will first give a summary of the traces of matrices of symmetry operations in three dimensions. This will be of importance when explaining how to calculate normal modes using symmetry. We will follow the procedure of G. Felder, [Fel16], with the notation of Jacobs University [Uni23] [GTW95]:

Table 1: Summary of the most general traces of different isometries [Bro+16].

Operation	Trace
Rotation about $\frac{2\pi}{n}$	$2cos(\frac{2\pi}{n}) + 1$
Reflection	1
Improper rotation about $\frac{2\pi}{n}$	$2cos(\frac{2\pi}{n}) - 1$
Identity	3
Inversion	-3

3.1 Linear crystals

For the linear crystals, we will restrict ourselves to a few special cases in order to introduce the reader into the topic of point groups. A more general case will be elaborated for the crystals in a toroidal confinement. We will also restrict ourselves to isometries respecting the shape of our cylindrical confinement. We assume to have a total of N ions, confined by an additional external force pointing in the $\pm z$ direction.

3.1.1 String crystals

For a linear crystal in one dimension embedded into 3 dimensions, the ions are aligned along the z-axis with equidistant spacing a. The symmetry operations are as follows:

- One proper ∞-fold rotation axis along the z-axis.
- One improper ∞-fold rotation axis along the z-axis and reflection in the xy-plane.
- Infinitely many proper 2-fold rotation axis perpendicular to the z-axis at $z = 0$.
- Infinitely many vertical mirror planes spanned by the z-axis.
- Inversion.
- Identity.

The symmetry group is $D_{\infty h}$ with order $h = \infty$. This group is of special interest, since linear molecules, such as carbon dioxide and beryllium hydride are also described by it.

The fixpoints for all operations are listed, for the two cases N odd or even, in table 2:

Table 2: Overview of the fixpoints for a string crystal of N particles under various isometries.

Operation	N even	N odd
E	N	N
I	0	1
C_∞	N	N
σ_v	N	N
S_∞	0	1
C_2	0	1

3.1.2 Zigzag crystals

Moving on to the 2-dimensional crystals embedded into 3-dimensional space, we find both the even and odd Zigzag patterns. The even Zigzag/ladder consists of two parallel strings, where every second particle of each string share the same z-position. The odd Zigzag/trestle is the same as the even Zigzag, except one string is translated along the z-direction about half the particle spacing. For simplicity, we will consider both cases with an even number of $N \geq 4$ ions.

The symmetry operations of the even Zigzag crystal are:

- One proper 2-fold rotation axis along the z-axis.
- One proper 2-fold rotation axis along the x-axis.
- One proper 2-fold rotation axis along the y-axis.
- One reflection along the xy-plane.
- One reflection along the yz-plane.
- One reflection along the xz-plane.
- Inversion.
- Identity.

Its group, D_{2h}, is of order $h = 8$ and the same as a rectangle embedded in three dimensions. The fixpoints of all these are listed in table 3:

Table 3: A summary of the fixpoints of isometries for the even Zigzag pattern.

Operation	N even $N \bmod 4 = 0$	N even $N \bmod 4 \neq 0$
E	N	N
I	0	0
$C_2(x)$	0	2
$C_2(y)$	0	0
$C_2(z)$	0	0
σ_{xy}	0	2
σ_{xz}	N	N
σ_{yz}	0	0

For the odd Zigzag pattern, the particles of the second string are shifted by half the spacing of the particles of the first string along the z direction. For this setup, we find the symmetry operations:

- One proper 2-fold rotation axis along the y-axis.
- One reflection along the x,z plane.
- Inversion.
- Identity.

These symmetries are described by the point group C_{2h}, which consists of a total of $h = 4$ elements. The fixpoints are listed below in table 4:

Table 4: A list of the fixpoints for the odd Zigzag under different isometries.

Operation	N even
E	N
I	0
$C_2(y)$	0
σ_v	N

3.1.3 Helical crystals

As mentioned above, we will only consider one helix - namely a double helix with $N = 12$, $n = 6$ and $k = 2$. The symmetry operations are as follows:

- Two proper 2-fold rotation axis in the xy-plane.
- One proper 2-fold rotation axis along the z-axis.
- Identity.

The corresponding symmetry group is D_2 with $h = 4$ elements and only N fixpoints for the identity operation.

3.2 Circular crystals

For the following discussion, we will consider a toroidal confinement centered around the origin. Here, we will remain in cartesian coordinates. Once again, we demand our isometries to respect the shape of the toroidal confinement.

3.2.1 String crystals

At low particle densities, the N ions will arrange equidistantly along the center circle of the torus with equal spacing. The symmetry group of this crystal, D_{Nh}, consists of the following elements:

- One N-fold rotation axis through the z axis.
- N vertical mirror planes through an ion and the opposite gap for N odd or between two opposite gaps/ions for N even.
- One horizontal mirror plane on the x,y plane.
- N two-fold rotation axis in the x,y plane.
- An improper rotation axis through the z axis.
- Inversion, if N even.
- Identity.

Similarly, the symmetry group of the next crystal, the even ZigZag of N ions, obeys the symmetry of $D_{\frac{N}{2}h}$, meaning all above considerations apply. The fixpoints for $D_{Nh}/D_{\frac{N}{2}}$, with order $h = 4N/h = 2N$ are listed in table 5 and 6:

Table 5: The fixpoints for isometries of the circular string pattern.

Operation	N even	N odd
E	N	N
I	0	–
$C_N(z)$	0	0
σ_h	N	N
σ_v	2	1
S_N	0	0
C_2	2	1

Table 6: The fixpoints for isometries of the even Zigzag pattern.

Operation	$N/2$ even	$N/2$ odd
E	N	N
I	0	–
$C_{N/2}(z)$	0	0
σ_h	N	N
σ_v	4	2
$S_{N/2}$	0	0
C_2	4	2

3.2.2 Odd Zigzag crystals

Moving on to the odd Zigzag pattern with N even particles, we find half of them aligned along an inner circle, with the other half aligned on an outer circle around them. They are separated by an angle $\frac{2\pi}{N}$ with alternating positions. The symmetry operations are listed below:

- One $N/2$-fold rotation axis through the z axis.
- $N/2$ vertical mirror planes.
- $N/2$ two-fold rotation axis in the x,y plane.
- An improper rotation axis through the z axis.
- Inversion, if $N/2$ even.
- Identity.

The corresponding point group is $D_{\frac{N}{2}h}$ with $h = 4\frac{N}{2}$ elements. The fixpoints are displayed in the following table 7:

Table 7: The fixpoints of the circular odd Zigzag pattern under its isometries.

Operation	-
E	N
I	0
σ_v	2
C_2	2
S_N	0
σ_h	N

3.2.3 Helical crystals

The most complex crystal is the helical crystal in the toroidal confinement. This time, however, we will consider the most general helix of N ions, n strings - of which k are parallel. Furthermore, we will assume that one particle of the helix is positioned on the xy-plane. The operations are listed in table 8:

Table 8: The (number of) isometries for a helix of N particles, n strings, of which k are parallel and the conditions for the isometries to exist.

Operation	Condition	Elements
E	–	1
$C_{\frac{N}{n}}(z)$	–	$N/n-1$
σ_v	$n=k$ or $n=2k$	N/n
C_2	-	N/n
I	N/k even $n=k$ or $n=2k$	1
$S_{\frac{N}{n}}$	$n=k$ or $n=2k$	N/n

First we will introduce some nomenclature to ease the following explanations about the aforementioned conditions and number of elements. The number of sites is defined as $s \coloneqq N/k$ and the number of repetitions $r \coloneqq N/n$. Furthermore, each site containing particle(s) located in the xy-plane on the outer most circle of the torus, will be referred to as a "start-site". We will mention regular polygons a few times in the explanation. With this phrasing we include the case of 2 corners, although these are technically no polygons.

The reason for the rotation around the z-axis is trivial when considering the fact that the full helix consists of one section repeating itself r times.

For the vertical mirror, σ_v, we can either have a mirror through the plane spanned by a site or a plane between two consecutive sites. This is possible either if $n=k$ or $n=2k$. Although the first case is trivial, for the second we need to ensure that the mirror does not reach the gap between points on the opposite site. This is fixed, however, by realising that $s=N/k=2N/k$ has to be even.

To understand why the number of C_2 rotations is exactly r, we need to realise that the rotation axis has to lie in the xy-plane and has to go through a section with at least one particle on the axis or be a section that is rotated by an angle of π/k compared to a start-site. The other option would be that the rotation axis passes through an imaginary site between two sides, where the imaginary site is again a section that is rotated by π/k compared to a start-site. Also, for this case, the antecedent/subsequent sites need to be turned clockwise/anticlockwise about the same angle with respect to the imaginary site along the beamline. These situations show up exactly r times in each setup. The first case happens exactly $r/2$ times if r is even. For these, the axis passes through two opposite start-sites. The remaining $r/2$ are perpendicular to the first ones and pass through two π/k rotated real or imaginary sites opposite to each other. If r is odd, we have a total of r rotation axis through start-sites, where opposite to it we have either a real or imaginary site rotated by π/k depending on whether the number of sites belonging to one repetition (n/k) is even or odd.

For the inversion, we postulated s to be even, since each site needs a counterpart. It is also obvious that we require r to be even, since we need each start-site to have a counterpart, however this condition is automatically fulfilled by our second demand. Let us take a closer look on how an inversion acts on a site, that is rotated by an angle with respect to a start-site: The inversion projects this site onto the other side of the torus while rotating it in the opposite direction about the same angle along the beamline - that is except for a permutation. Since each site is rotated along the beam line in the same direction with respect to a start-site - this is how our helices are constructed - we must require $n=k$ or $n=2k$ for an inversion to be possible.

For the improper rotations, we require each start-site to land on a different start-site after the operation. This gives a constraint on the angle, about which rotation is possible - namely $2\pi/r$. Furthermore, we require the horizontal reflection to be possible. The decisive thought is, that a regular polygon can only be reflected along a plane, if it is a start-site or is rotated about an angle π/k compared to a start-site.

Taking these operations into account, we end up with the point groups D_2, if we have no horizontal reflection and D_{rh} otherwise. The first one has a total of $h = 4$ elements, whereas the second one contains $h = 4r$ elements.

If s is odd, clearly each vertical mirror has to fix exactly k points belonging to the site the mirror passes through. On the other hand, if s is even, we need to distinguish between the cases $n = k$ and $n = 2k$. For the first case, we also have r even which implies that the mirror either passes through two sites or no site at all, giving $2k$ or 0 fixpoints. The second case also requires r to be even, however it restricts us to only one mirror through two sites - $2k$ fixpoints.

The horizontal mirror is the only special case of an improper rotation, which contains fixpoints. Clearly, the fixpoints for the aforementioned cases $n = k$ and $n = 2k$ are $2r$ if n is even and r if n is odd. To imagine this, the reader is advised to consider one repetition of strings as an "effective" polygon of n corners. If n is even, a total of 2 corners will lie on the plane per repetition. For n odd, an analog thought applies.

Once again, the most complex cases are the C_2 rotations. To sum up the fixpoints of the aforementioned possibilities for these rotations, the following flowchart is provided in figure 7. We will give a quick explanation for this: A C_2 rotation axis passing through a start-site will always fix 2 points, if k is even and 1 point if k is odd. A start-site rotated by π/k will fix 0 points if k is even and 1 if k is odd.

Figure 7: A flowchart of the fixpoints during a C_2 rotation of a circular helix.

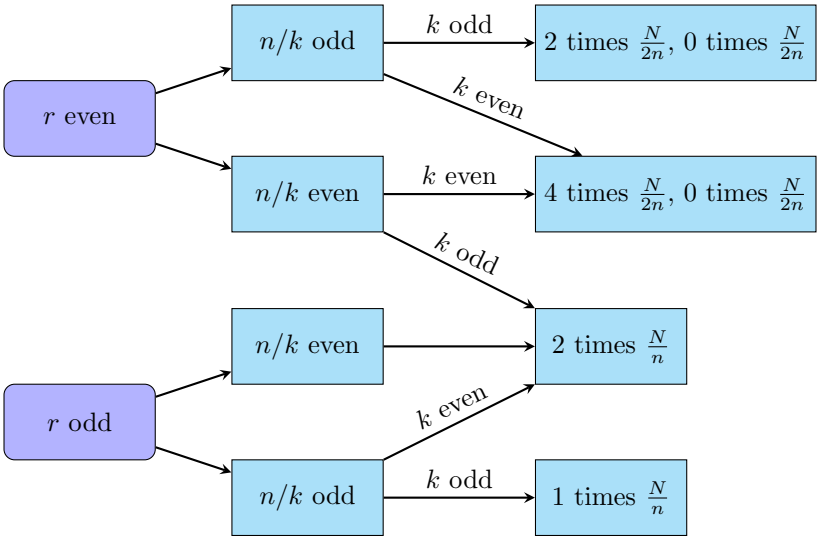

3.2.4 Normal modes

By using the character tables of point groups, the normal modes of crystals with rotationally invariant potential, which is not true for crystalline beams, can be determined. We will demonstrate this using the point groups found above. For this, we need to decompose the representation $\rho(g)$, which projects each particle onto another one, followed by a permutation counteracting the initial switching, into its irreducible representations. The character of each element $g \in G$ under ρ can be obtained by multiplying the trace 1 of a representative of each conjugacy class with its corresponding number of fixpoints. Using the orthogonality relation,

$$(\chi_\rho, \chi_j) = \frac{1}{|G|} \sum_{g \in G} \overline{\chi_\rho(g)} \chi_j(g),$$

and subtracting the irreducible representations, which are not translational or rotational invariant, the decomposition can be found and is listed below for a few examples in table 9.

Table 9: Examples of normal modes of different crystals.

	Crystal	Parameters	Normal modes
Linear crystals	String	$N = 5$	$2A_{1g} + E_{1g} + 2A_{1u} + 2E_{1u}$
	Even Zigzag	$N = 6$	$3A_g + B_{1g} + 2B_{2g} + +A_u + 2B_{1u} + B_{2u} + 2B_{3u}$
	Odd Zigzag	$N = 8$	$7A_g + 2B_g + 3A_u + 6B_u$
	Helix	$N = 12, n = 6, k = 2$	$9A + 7B_1 + 7B_2 + 7B_3$
Circular crystals	String	$N = 3$	$A_1' + E'$
	Even Zigzag	$N = 6$	$2A_1' + A_2' + 3E' + A_2'' + E''$
	Odd Zigzag	$N = 6$	$2A_1' + A_2' + 3E' + A_2'' + E''$
	Helix	$N = 12, n = 6, k = 3$	$6A_g + 3B_{1g} + 3B_{2g} + 3B_{3g} + 2A_u + 5B_{1u} + 4B_{2u} + 4B_{3u}$

3.3 Landau theory of phase transitions

Landau theory provides an elegant way to gain deeper insights into the transitions between phases of solid matter. By expanding the thermodynamic potential Φ as a function of the systems order parameter, while at the same time handling the systems symmetries, a bridge between group theory - for crystals - and thermodynamics can be build [Ili11].

For crystals, the order parameter is usually chosen to be or is closely related to the Fourier modes of the transformed mass density.

$$\rho(\vec{x}) = \sum_{\vec{k}} \rho_{\vec{k}} e^{\frac{2\pi i}{L} \vec{k} \cdot \vec{x}}.$$

We will proceed by expressing the density as a linear combination of the irreducible representations of the symmetry group (G_0) of the high-symmetry state:

$$\delta\rho = \sum_n{}' \sum_{\vec{k}} \eta_{\vec{k}}^{(n)} \chi_{\vec{k}}^{(n)}.$$

Here, the first sum goes over all irreducible representations and we leave out the one-dimensional unit representation, which is indicated by the prime in the sum. The coefficients can be calculated using the projector,

$$P_\alpha \rho(\vec{x}) = \frac{d_\alpha}{|G|} \sum_{g \in G} \overline{\chi^{(\alpha)}(g)} \hat{g} \rho(\vec{x}),$$

where d_α is the dimension of the irreducible representation and $\hat{g}$ is the action of the group element g. Finally the thermodynamic potential can be obtained by expansion around the order parameter:

$$\Phi = \Phi_0 + \sum_n{}' A^{(n)}(p, T) \sum_{\vec{k}} \left[\eta_{\vec{k}}^{(n)}\right]^2 + \cdots \tag{10}$$

Since we have taken the number of particles constant, finitely many helices are possible to appear. This low-symmetry phase is described by a group G. Our previous analysis restricted ourselves to the groups D_{Nh}, $D_{\frac{N}{2}h}$, $D_{\frac{N}{n}h}$ or D_2. Each of these has a number of irreducible representations, for D_2 it is $l = 4$. For D_{Nh} it is either $l = N+6$, if N is even and $l = N+3$ otherwise.

Finally, since the phase transition only depends on the (negative) n-th coefficient n, we can define the order parameter to be,

$$\eta^2 = \sum_{\vec{k}} \left[\eta_{\vec{k}}^{(n)}\right]^2,$$

and apply some treatment to our expansion 10, to obtain our final result:

$$\Phi(p,T) = \Phi_0(p,T) + \tilde{a}(p)(\Delta T)\eta^2 + a_4(p)\eta^4. \tag{11}$$

By varying the initial conditions of our system at constant ion charge, temperature and focusing constant, we may measure Φ and η and fit these points using our expansion. From this we can determine the dependence of our order parameter on the systems parameters, $\eta_{\vec{k}}^{(n)} = \eta_{\vec{k}}^{(n)}(Q, k', T)$, and therefore the thermodynamic potentials dependence on the system parameters. Each of the minima in the potential will now correspond to one of our low-symmetry groups G.

This procedure can now be compared to formula 5 when applied to a helix in the toroidal confinement with N fixed and n, k arbitrary. For this, we first need to point out a condition. In order to apply eq. 5 for a stability analysis, we need the confinement to have a small curvature compared to the length of each of the r repetitions. This is demanded with the condition $R \gg a'$, with $a' = \frac{2\pi nR}{N}$. Furthermore, we know that in the ordered state, a total of n strings, each with periodicity N/n per revolution will emerge. This translates to a frequency $f = N/2\pi nR$ m^{-1}, which is the inverse of a'.

4 Numeric results

For the numeric part of our analysis, we focused on two different setups. The first one was used to simulate an infinitely long crystalline beam in one spacial direction. To achieve this, the above equations of motion (eq. 3 and 4) were integrated in $(0.0, t_{end})$ using the Leap frog algorithm, which is of second order and stable for oscillatory motion [BL18]. This algorithm proved to be sufficient to replicate important results of prior research. Furthermore, particles moved freely in 3 dimensional euclidean space, with the exception of periodic boundary conditions along the z-axis. For this, the particle positions were checked and updated after every time step. Finally each particle was exposed to Coulomb repulsion by every other "real" particle and its "imaginary" counterpart, placed on the other side of the boundary.

For the circular confinement simulation, obeying the equations of motion, the standard integrator Tsitouras 5/4 Runge-Kutta was chosen.

In both setups, crystallisation was demonstrated. The linear crystals displayed phase transitions at the expected linear densities λ. All helical structures could be described by the parameters N, n and k. Furthermore, crystals are usually Doppler cooled by two forces of the form:

$$\vec{F} = \hbar\vec{k}\frac{\Gamma}{2}\frac{I/I_{sat}}{1 + I/I_{sat} + 4\delta^2/\Gamma^2}, \tag{12}$$

with frequency detuning from resonance $\delta = \omega - \omega_0 + \vec{k}\cdot\vec{v}$. Both approximate the force of a photon beam with photon wave number $\vec{k}$, intensity I and saturated intensity I_{sat}. In our setup, the photon beams are counterpropagating and the lower beam has a time dependent frequency $\omega = \omega(t)$, which results in a total force [And+13] [Foo04]:

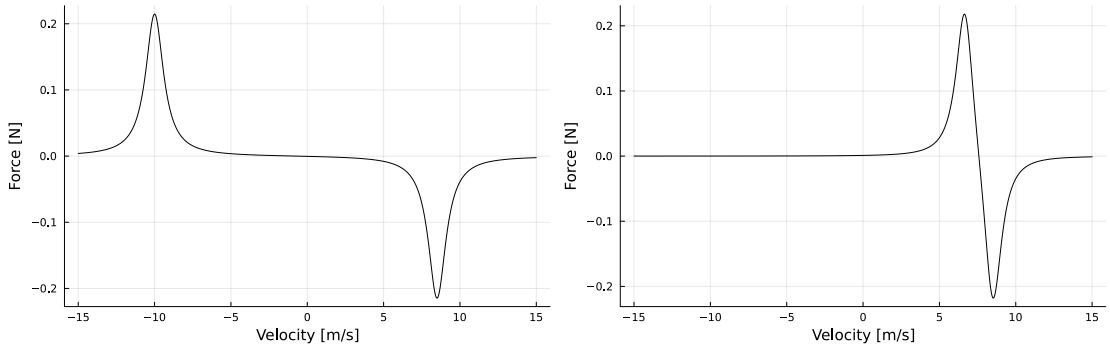

Figure 8: The resulting average force of two counterpropagating beams on a moving particle. The left figure depicts the start of the acceleration process, the right figure the end of it. Amplitudes and frequencies were chosen arbitrarily.

The following plots depict examples of crystallisation in both the linear and circular confinements. Also, for the linear case, we have included the Doppler force from the counterpropagating beams:

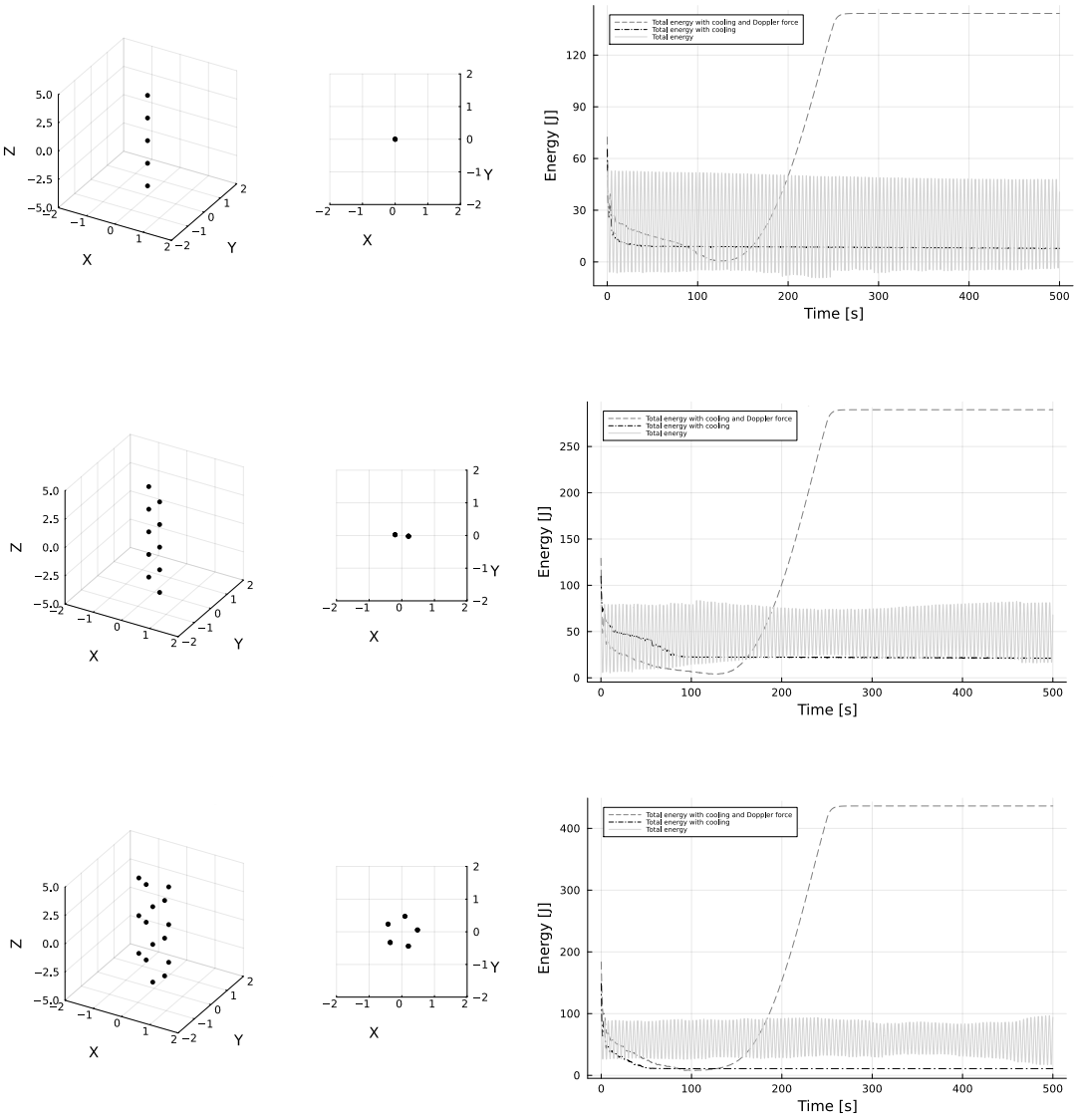

Figure 9: Left: Examples of linear crystalline ion beams, of $N = 5, 10, 15$ ions, with electric charge $Q = 1.5$ C, spring constant $k = 0.6\ \mathrm{N\,m^{-1}}$, mass 1.0 kg and breaking constant $\alpha = 0.3\ \mathrm{kg\,s^{-1}}$ on the domain $z \in [-5.0; 5.0]$. Right: The energies of each beam (eq. 1), depending on whether the ions were cooled and/or accelerated as in eq. 12.

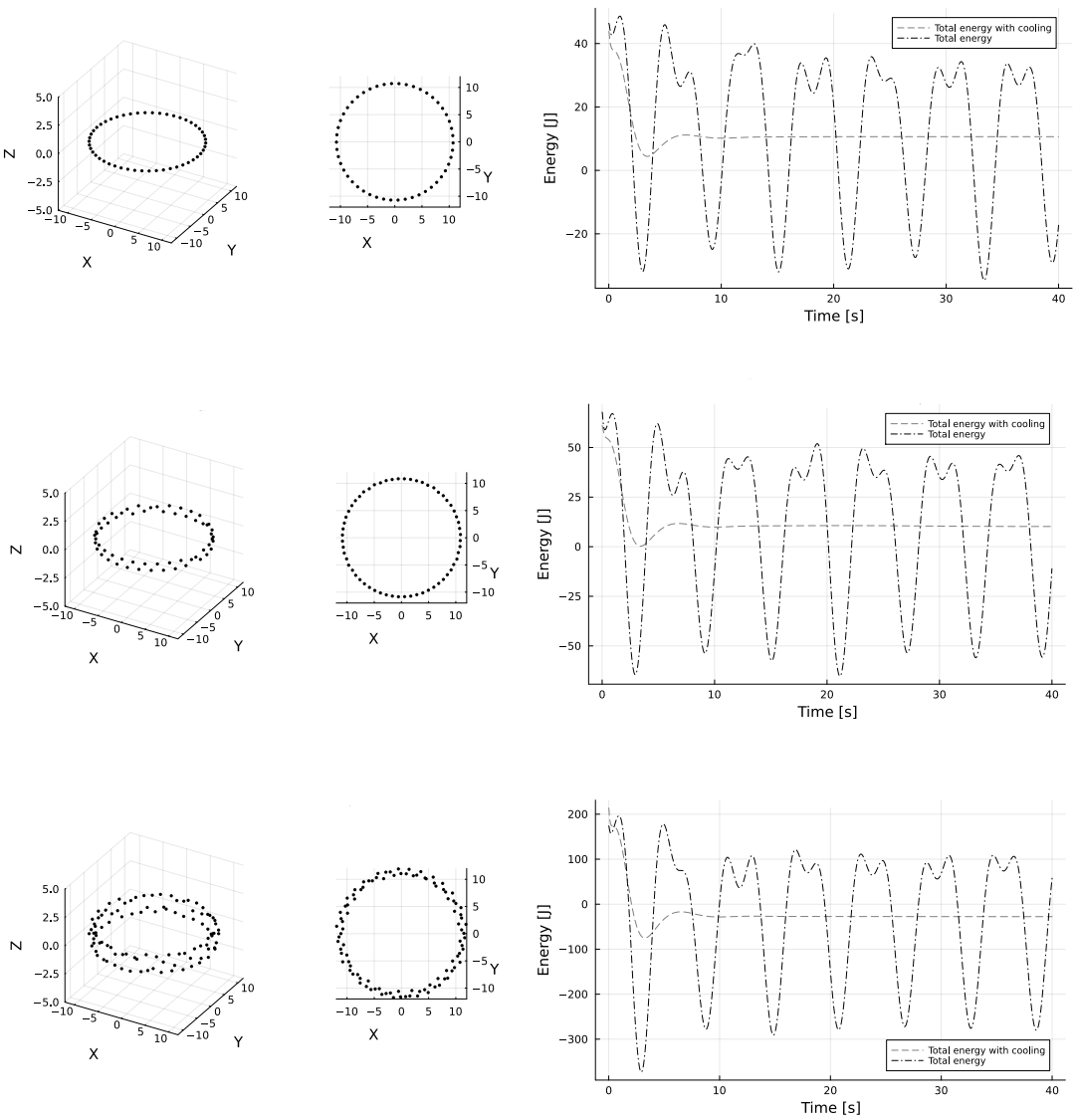

Figure 10: Left: Examples of circular crystalline ion beams, of $N = 50, 60, 100$ ions, with electric charge $Q = 2.0$ C, spring constant $k = 1.0\ \mathrm{N\,m^{-1}}$, mass 1.0 kg and breaking constant $\alpha = 1.0\ \mathrm{kg\,s^{-1}}$ in a toroidal confinement with radius $R = 10.0$ m. Right: The energies (eq. 2) of each beam, depending on whether the ions were cooled.

5 Discussion

By using numeric methods, we replicated findings of the past and elaborated on their validity. We have also presented different points of views on the topic of crystalline ion beams. Although these approaches seemed to be chosen randomly at first glance, Landau theory of phase transitions combines them in an elegant way.

For the stability analysis, we focused on the stability of helices for arbitrary N, n and k and provided an approximation of the electric field of a general helix. For eq. 5 to be used in a toroidal confinement, condition $R \gg a'$ needs to hold, which is likely but has to be tested in an actual storage ring. Furthermore, the use case for the approximation of the electric field (eq. 9) of a helix is questionable. Numeric methods might prove to have a better efficiency/exactness ratio when calculating the electric fields of helices directly. It could, however, prove to be useful when calculating the force on the particles on one side of the storage ring from the particles on the opposite side.

Our group theoretical treatment gave insights into the geometric structure of linear and circular helices. Although the approach presented to calculate normal modes is not of specific interest when considering ion beams, since these beams are not confined by internal forces, our results may find applications in other areas of research. These results did and will, however, play a crucial role when applying Landau theory. An exact understanding of the underlying group of different crystals will help to expand the thermodynamic potential correctly. Consequently, the fitting of the thermodynamic potential and the stability regions will be more exact. This procedure, as well as eq. 5, can be used when the crystal does not differ a lot from the ordered state. In the Landau case, this is due to the "breaking off" point of the expansion, whereas in the second case, the specific geometry of the problem is decisive.

Finally, our description of Landau's theory of phase transitions gave an introductory insight into the topic, but needs to be treated either numerically or experimentally to provide more insight into the structure of the thermodynamic potential (eq. 12). From this, thermodynamic tools may be used to dive deeper into the topic of classical statistical mechanics.

6 Outlook

For a future analysis, the point group of the Zigzag in the circular confinement, as well as the linear helix could be of interest. For the Zigzag pattern, the cases in which not all particles are located on the xy-plane, should be taken into consideration. Furthermore, by introducing the curvature and moving to the relativistic regime, a more precise understanding of old and new effects could be established. Finally, simulating realistic electric fields such as in an actual circular rf storage ring, might give more insight on the stability of the beams.

References

[GTW95] Achim Gelessus, Walter Thiel, and Wolfgang Weber. "Multipoles and symmetry". In: *Journal of chemical education* 72.6 (1995), p. 505.

[Rug00] Alessandro G Ruggiero. "Crystalline beams". In: *The Physics Of High Brightness Beams*. World Scientific, 2000, pp. 124–145.

[SSH01] T Schätz, U Schramm, and D Habs. "Crystalline ion beams". In: *Nature* 412.6848 (2001), pp. 717–720.

[Cha02] Alex W Chao. *Lecture notes on topics in accelerator physics*. Tech. rep. SLAC National Accelerator Lab., Menlo Park, CA (United States), 2002.

[Foo04] Christopher J Foot. *Atomic physics*. Vol. 7. OUP Oxford, 2004.

[SH04] Ulrich Schramm and D Habs. "Crystalline ion beams". In: *Progress in particle and Nuclear Physics* 53.2 (2004), pp. 583–677.

[Ili11] Enej Ilievski. "LANDAU THEORY OF PHASE TRANSITIONS from group-theoretical perspective". In: (2011).

[And+13] Z Andelkovic et al. "Laser cooling of externally produced Mg ions in a Penning trap for sympathetic cooling of highly charged ions". In: *Physical Review A* 87.3 (2013), p. 033423.

[Ren15] Joseph M Renes. "Quantum information theory". In: *Lecture Notes, February* 4 (2015).

[Bro+16] Carolyn Pratt Brock et al. *International tables for crystallography volume A: Space-group symmetry*. Wiley Online Library, 2016.

[Fel16] Giovanni Felder. "Mathematische methoden der physik ii". In: *ETH Zürich, June* (2016).

[BL18] Charles K Birdsall and A Bruce Langdon. *Plasma physics via computer simulation*. CRC press, 2018.

[Bru+19] Colin D Bruzewicz et al. "Trapped-ion quantum computing: Progress and challenges". In: *Applied Physics Reviews* 6.2 (2019).

[Uni23] Jacobs University. *Character tables for chemically important point groups*. 2023. URL: http://symmetry.jacobs-university.de/ (visited on 07/07/2024).

7 Appendix

We display some of the aforementioned character tables of the groups relevant for our discussion [Uni23].

Table 10: Character table for point group $D_{\infty h}$.

$D_{\infty h}$	E	$2C_\infty$	...	$\infty\sigma_v$	i	$2S_\infty$	...	$\infty C_2'$
A_{1g}	1	1	...	1	1	1	...	1
A_{2g}	1	1	...	-1	1	1	...	-1
E_{1g}	2	$2\cos(\phi)$	...	0	2	$-2\cos(\phi)$	...	0
E_{2g}	2	$2\cos(2\phi)$	...	0	2	$2\cos(2\phi)$	...	0
E_{3g}	2	$2\cos(3\phi)$	...	0	2	$-2\cos(3\phi)$	...	0
E_{ng}	2	$2\cos(n\phi)$	...	0	2	$(-1)^n 2\cos(n\phi)$	...	0
...	...	...	...	...	...	...	...	...
A_{1u}	1	1	...	1	-1	-1	...	1
A_{2u}	1	1	...	-1	-1	-1	...	-1
E_{1u}	2	$2\cos(\phi)$	...	0	-2	$2\cos(\phi)$	...	0
E_{2u}	2	$2\cos(2\phi)$	...	0	-2	$-2\cos(2\phi)$	...	0
E_{3u}	2	$2\cos(3\phi)$	...	0	-2	$2\cos(3\phi)$	...	0
E_{nu}	2	$2\cos(n\phi)$	...	0	-2	$(-1)^{n+1} 2\cos(n\phi)$	...	0
...	...	...	...	...	...	...	...	...

Table 11: Character table for point group D_{2h}.

D_{2h}	E	$C_2(x)$	$C_2(y)$	$C_2(z)$	i	$\sigma(xy)$	$\sigma(xz)$	$\sigma(yz)$
A_g	1	1	1	1	1	1	1	1
B_{1g}	1	1	-1	-1	1	1	-1	-1
B_{2g}	1	-1	1	-1	1	-1	1	-1
B_{3g}	1	-1	-1	1	1	-1	-1	1
A_u	1	1	1	1	-1	-1	-1	-1
B_{1u}	1	1	-1	-1	-1	-1	1	1
B_{2u}	1	-1	1	-1	-1	1	-1	1
B_{3u}	1	-1	-1	1	-1	1	1	-1

Table 12: Character table for point group C_{2h}.

C_{2h}	E	$C_2(z)$	i	σ_h
A_g	1	1	1	1
B_g	1	-1	1	-1
A_u	1	1	-1	-1
B_u	1	-1	-1	1

Table 13: Character table for point group D_2.

D_2	E	$C_2(z)$	$C_2(z)$	$C_2(z)$
A	1	1	1	1
$B1$	1	1	-1	-1
$B2$	1	-1	1	-1
$B3$	1	-1	-1	1